J. Fluid Mech. (1992), *vol.* 241, *pp.* 59–74
Printed in Great Britain

Natural convection and dispersion in a tilted fracture

By ANDREW W. WOODS[1] AND STEFAN J. LINZ[2]

[1] Institute of Theoretical Geophysics, Department of Applied Mathematics and Theoretical Physics, University of Cambridge, Silver Street, Cambridge CB3 9EW, UK

[2] Department of Engineering Sciences and Applied Mathematics, Northwestern University, Evanston, IL 60208, USA

(Received 26 March 1991 and in revised form 2 January 1992)

In many geophysical situations, fluid is contained in long narrow fractures embedded within an impermeable medium of different thermal conductivity; and there may be a uniform vertical temperature gradient imposed upon the system. We show that whenever the slot is tiled to the vertical, convection develops in the fluid, even if the background temperature increases with height. We then investigate the transport of passive material governed by this flow. The dispersion coefficient of a passive contaminant transported by this flow $D_T = f[R \sin^2\phi]\kappa^2 \cot^2\phi/D$, where κ and D are the thermal and compositional diffusivities, ϕ is the angle of tilt and R is a Rayleigh number for the slot.

Using typical values for the physical properties of a water-filled fracture, we show that the Earth's geothermal gradient produces a convective flow in a fracture through the mechanism above; this has an associated dispersion coefficient $D_T \sim 10^2$–$10^3 D$ in fractures about a centimetre wide. We show that this shear dispersion could transport radioactive material, of half-life 10^4 years, tens of metres along the fracture within one half-life; without this dispersion, the material would only diffuse a few metres along the fracture within one half-life.

If there is a background salinity gradient along the slot in addition to the thermal gradient, analogous steady flow solutions exist; if the flow is stable, the salinity may either enhance or reduce the steady flow and associated dispersion of passive tracer.

1. Introduction

In many geophysical situations, fluid is enclosed in long narrow slots, for example in porous layers of sandstone embedded in shale; in water trapped in narrow fissures in the upper crust; in cooling joints embedded in rock or in tunnels leading to flooded underground caves/mines. It is of considerable interest to understand the different modes of natural convection which may arise in these slots in order to understand the transport and rate of spread of passive contaminants. For example, radioactive material buried deep in the Earth may be dispersed to the surface through convection in a tilted, water-filled fracture much more rapidly than by natural diffusion. Such convective transport may also significantly reduce the timescale of diagenesis; material, in solution, may be transported through porous sandstone layers convectively and precipitate out of solution as it enters a cooler region, thereby changing the structure of the sandstone over a much shorter timescale than would be caused by molecular diffusion (Bjorlykke 1989; Davis *et al.* 1985).

In this contribution, we describe an important natural convective flow which

arises in a tilted, fluid-filled slot embedded in an impermeable medium of different thermal conductivity. We show that whenever there is a background vertical temperature gradient, a convective flow will develop. The flow arises irrespective of whether the temperature increases or decreases with depth. This flow may therefore develop even in situations which are stable to Rayleigh–Bénard convection.

Davis *et al.* (1985) have shown that a similar type of flow develops in a permeable rock, although in the different geometry of a domed sheet. Our flow is a generalization of the flow described by Phillips (1970) and Wunsch (1970), who showed independently that a tilted insulating boundary at the edge of a stratified fluid drives a flow because the isopycnals at the boundary must be normal to the boundary. Therefore, the isopycnals are not horizontal and the associated pressure gradient drives a flow. In the present situation, the boundaries are conducting and so one might consider that the isopycnals within the fluid could be horizontal. However, we show below that there is no steady static solution, except when the slot is either horizontal or vertical, or if the thermal conductivity of the fluid and surrounding medium are the same. We calculate and describe our new flow solutions and distinguish the cases in which the background temperature gradient is stabilizing or destabilizing.

Using our flow solution we calculate the Taylor (1953) dispersion coefficient of a passive material carried by the flow. We investigate the dependence of the dispersion coefficient upon the angle of tilt and also upon the slot Rayleigh number. We then apply these results to investigate the transport of a passive tracer through a rock fracture. In particular, we examine the maximum concentration of a radioactively decaying material as a function of the distance along the fracture from the source.

If there is also a salinity gradient along the fracture, then following Chen (1974), we show that our present analysis may be readily generalized to describe steady double-diffusive flows.

2. Proof of the existence of flow

Consider a two-dimensional slot with angle of tilt ϕ with respect to the horizontal, width d and with slot coordinates (η, ξ) as shown in figure 1. In the solid in the far field there is a uniform vertical temperature gradient, $T_z = G$. Continuity of temperature and normal heat flux at the interface between the solid and the incompressible liquid, at $\eta = \pm\frac{1}{2}d$ requires

$$k_s T_\eta\Big|_{\eta+} = k_\ell T_\eta\Big|_{\eta-} \quad \text{at} \quad \eta = \pm\tfrac{1}{2}d \tag{1}$$

and

$$T\Big|_{\eta+} = T\Big|_{\eta-} \quad \text{at} \quad \eta = \pm\tfrac{1}{2}d, \tag{2}$$

where k_ℓ and k_s represent the thermal conductivity of the liquid and solid. Since the isotherms in the solid may curve, it is not immediately clear that those in the liquid cannot remain horizontal and a steady no-flow solution develop. However, if this were possible, then continuity of temperature from one side of the fracture to the other would require $T_\eta = G\cos\phi$ along both the lines AB and CD in figure 2, where CD is chosen to be sufficiently far from the slot that the isotherms through CD are horizontal. If the slot is sufficiently long, then the heat flux across AD equals that through BC. Therefore, for a steady solution, the heat flux across AB must equal that

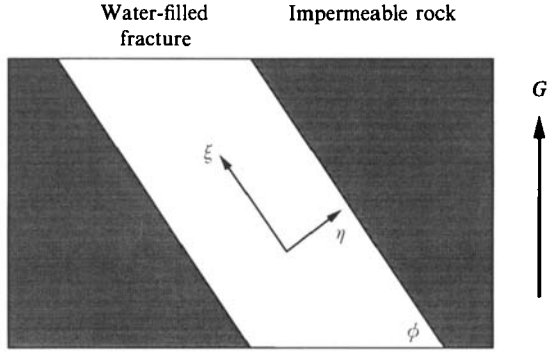

FIGURE 1. Schematic of fracture geometry showing coordinate system.

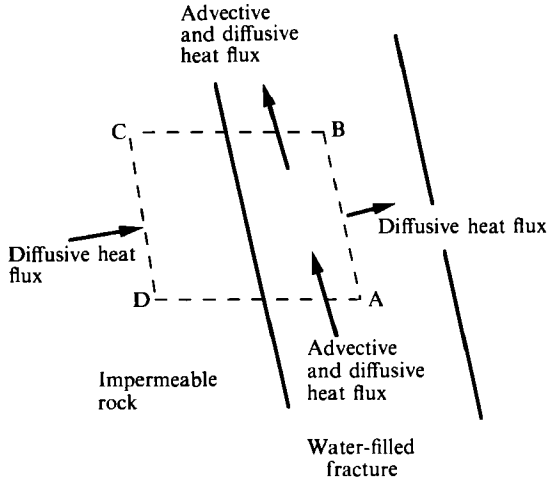

FIGURE 2. Diagram of a control volume ABCD through which there is no heat flux in steady state. The sum of the advective and diffusive fluxes through the boundaries AD and BC are equal, requiring the diffusive flux through AB and CD to match. AB and CD are parallel to the walls of the fracture.

across CD. This is not possible if the thermal conductivities of the solid and fluid differ and $T_\eta = G\cos\phi$. We conclude that there must be a flow.

Note that Davis *et al.* (1985) and subsequently Phillips (1991) have shown analytically that no zero-flow solution exists in an analogous problem concerned with tilted porous layers embedded in impermeable host rock. Our proof is an alternative, physical argument explaining why flow must develop,

3. The flow solution

The steady diffusion equation in the solid is satisfied if the isotherms in the solid are purely horizontal. In this case, to satisfy (1) the isotherms in the liquid at the sidewalls of the slot are not horizontal and there is a flow. In a long narrow slot, the flow is purely along the slot, $u = u(\eta)$. The motion is governed by the vorticity equation

$$\nu\frac{\partial^3 u}{\partial\eta^3} = -\alpha g\left(\frac{\partial T}{\partial\eta}\sin\phi - \frac{\partial T}{\partial\xi}\cos\phi\right), \tag{3}$$

where ν is the kinematic viscosity and we have assumed that the density varies linearly with temperature, $\rho = \rho_0(1-\alpha(T-T_0))$. We remark that for parallel flow, (3) is in fact the nonlinear vorticity equation. The equation for the conservation of heat is

$$u\frac{\partial T}{\partial \xi} = \kappa\left(\frac{\partial^2 T}{\partial \eta^2}+\frac{\partial^2 T}{\partial \xi^2}\right), \tag{4}$$

where $T(\xi,\eta) = T_0 + G\xi\sin\phi + \theta(\eta)$ is the temperature in the slot, with T_0 an arbitrary constant, G the imposed vertical temperature gradient in the solid and κ the thermal diffusivity of the fluid. We assume that κ, α and ν are constant. For simplicity we define $\theta(0) = 0$. The temperature in the solid is given by the continuity of normal heat flux, (1), and temperature, (2), at $\eta = \pm\frac{1}{2}d$, together with the imposed vertical gradient G. If we also impose the no-slip condition on the flow field at $\eta = \pm\frac{1}{2}d$ and introduce the dimensionless variable $\hat{\eta} = 2\eta/d$, then the flow solution is

$$u(\hat{\eta}) = \frac{8\kappa(\epsilon-1)\cot\phi}{d}\left[\frac{\gamma F(\hat{\eta};\gamma)}{\sin 2\gamma+\sinh 2\gamma}\right] \tag{5}$$

with the temperature field satisfying the equation

$$\theta(\hat{\eta}) = Gd\cos\phi\left[\tfrac{1}{2}\hat{\eta}+H(\hat{\eta};\gamma)\left(\frac{(\epsilon-1)}{\gamma(\sin 2\gamma+\sinh 2\gamma)}\right)\right], \tag{6}$$

where

$$\gamma^4 = \frac{\alpha g G d^4}{64\nu\kappa}\sin^2\phi, \tag{7}$$

$$F(\hat{\eta};\gamma) = \sin\gamma\cosh\gamma\cos\gamma\hat{\eta}\sinh\gamma\hat{\eta} - \cos\gamma\sinh\gamma\sin\gamma\hat{\eta}\cosh\gamma\hat{\eta}, \tag{8}$$

$$H(\hat{\eta};\gamma) = \sin\gamma\cosh\gamma\sin\gamma\hat{\eta}\cosh\gamma\hat{\eta} + \cos\gamma\sinh\gamma\cos\gamma\hat{\eta}\sinh\gamma\hat{\eta}, \tag{9}$$

and the constant ϵ is defined as the ratio of the thermal conductivities of the solid and liquid, $\epsilon = k_s/k_\ell$ and has a value in the range 1.5–3.0 in a water-saturated rock and 7–10 in an oil-saturated rock. We can define a slot Rayleigh number as

$$R = -\frac{\alpha g G d^4}{64\nu\kappa} \tag{10a}$$

and this gives the relationship

$$\gamma^4 = -R\sin^2\phi. \tag{10b}$$

We immediately deduce that four different flow regimes exist depending upon whether (i) the temperature in the rock increases ($G > 0$ and $R < 0$) or decreases ($G < 0$ and $R > 0$) with height; and (ii) whether the conductivity of the solid is greater ($\epsilon > 1$) or smaller ($\epsilon < 1$) than that of the liquid. The dimensionless velocity and temperature profiles (corresponding to the expressions in the large square brackets in (5) and (6)) for each case are shown in figure 3(*a–d*).These are most easily understood by comparing the four different temperature profiles with the dashed lines which represent the temperatures in the case in which the isotherms in the liquid are horizontal ($\epsilon = 1$). If the temperature solution shown by the solid line is greater than that of the dotted line then the fluid is hotter and hence rises; if the temperature is smaller than that given by the dotted line, then the fluid is colder and heavy and hence sinks. The flows in figure 3 are shown for $\gamma = 1$, which corresponds to a rather weak temperature gradient; for example, if $\phi = \frac{1}{4}\pi$, then we have $|R| = 2$.

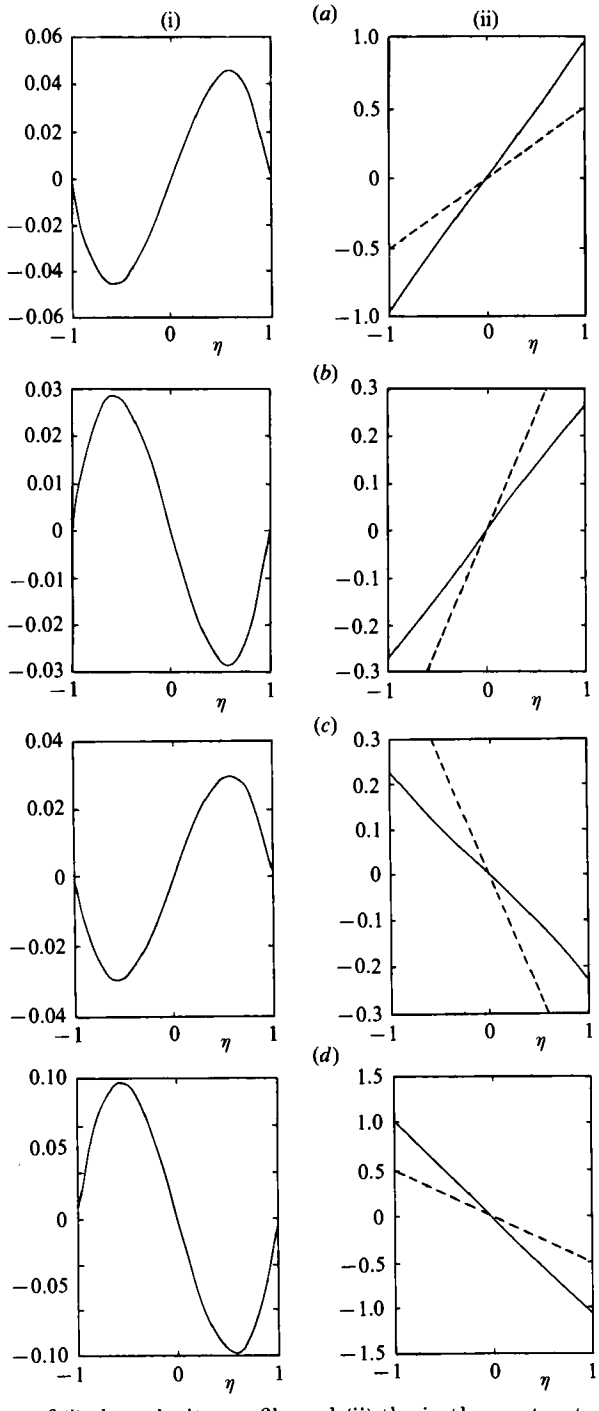

FIGURE 3. Diagram of (i) the velocity profile and (ii) the isotherm structure across the fracture in the four distinct cases (*a*) $\gamma = 1$, $G > 0$, $\epsilon = 2$, (*b*) $\gamma = 1$, $G > 0$, $\epsilon = 0.5$, (*c*) $\gamma = (-1)^{\frac{1}{4}}$, $G < 0$, $\epsilon = 0.5$ and (*d*) $\gamma = (-1)^{\frac{1}{4}}$, $G < 0$, $\epsilon = 2$.

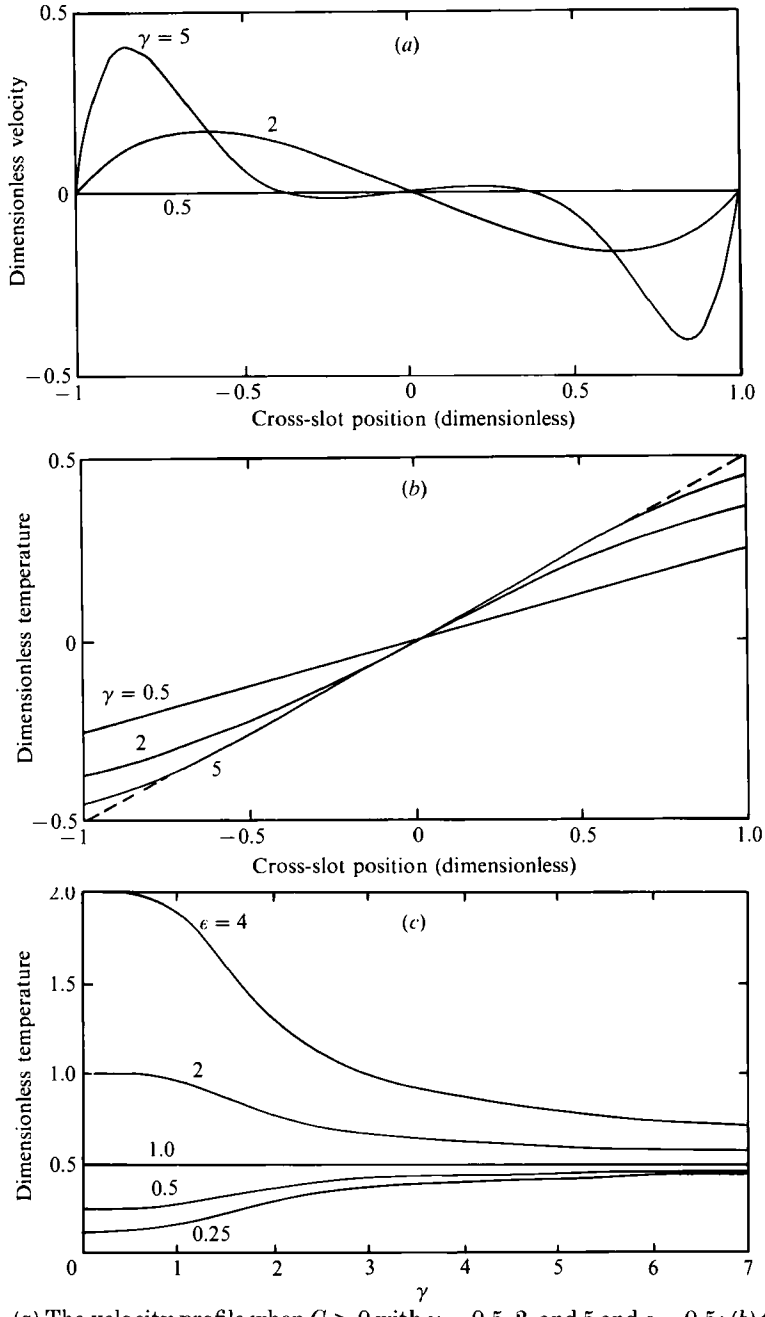

FIGURE 4. (*a*) The velocity profile when $G > 0$ with $\gamma = 0.5$, 2, and 5 and $\epsilon = 0.5$; (*b*) the temperature profiles corresponding to (*a*); and (*c*) the variation of the temperature on the upper side of the slot, $\hat{\eta} = 1.0$, as γ is increased for $\epsilon = 0.25$, 0.5, 1.0, 2.0 and 4.0. Note $\epsilon = 1.0$ gives no flow.

An important feature of these flows is that they scale with the thermal diffusivity of the fluid and are therefore rather weak; however, we show below that over long timescales they may play a very important role in transporting material with a smaller diffusion coefficient along the fracture. We also note that these flow solutions are exact nonlinear solutions. The flow disappears when the slot is horizontal, $\phi = 0$, or vertical, $\phi = \frac{1}{2}\pi$, and a purely diffusive solution obtains in the fluid; flow only arises

when the slot is tilted. By symmetry, there is no mean flow; a mean flow may develop when the two walls have different slopes as discussed by Woods (1991), in the rather different context of ocean mixing. The flows of figure 3 may be produced in the laboratory by applying a temperature gradient, $G\sin\phi$ along the walls of the slot and a horizontal temperature difference ΔT across the slot, where ΔT is given by

$$\Delta T = (\epsilon - 1)\, Gd \cos\phi \left(\frac{H(1,\gamma) - H(-1,\gamma)}{2\gamma(\sin 2\gamma + \sinh 2\gamma)} \right). \tag{11}$$

3.1. *The stable background temperature distribution*

When $G > 0$, and hence $R < 0$, the background temperature increases with depth and so the flow is stable. This is essentially because in the slot, hot and hence buoyant fluid overlies cold fluid (note we only consider fluids in which $\kappa \ll \nu$). The flow which develops tends to restore the isotherms in the fluid to the horizontal. The case in which $\epsilon < 1$ is a generalization of the flow discussed by Phillips (1970) and Wunsch (1970) and represents the situation in which the fluid is a good conductor of heat. The solution given as equations (23) and (24) by Phillips is recovered from (5) and (6) when $\epsilon = 0$; this limit represents the situation in which the surrounding material is insulating and is therefore relevant for convection induced by salinity gradients rather than temperature gradients. The case in which $\epsilon > 1$ represents the situation in which the fluid is a poor conductor; this situation may arise, for example, if the fluid is oil or, in a different situation, the surrounding material is metallic.

When the background temperature distribution is stable, γ (equation (7)) may be interpreted as the ratio of the slot width to the lengthscale across which the flow can restore the isotherms to the horizontal. Therefore, as the magnitude of the slot Rayleigh number, $|R|$, and hence $\gamma = (-R\sin^2\phi)^{\frac{1}{4}}$ increase the flow becomes confined to two independent boundary layers beside each wall; we demonstrate this phenomenon in figure 4(*a*) in which flow profiles are shown when γ equals 0.5, 2.0 and 5.0. Indeed, in figure 4(*b*), it may be seen that as γ is increased, the temperature gradient near the centre of the slot approaches the dashed line (which corresponds to the gradient in the surrounding rock where the isotherms are horizontal) and hence the isotherms become approximately horizontal except beside each boundary. In figure 4(*c*) we show that as γ increases and the flow becomes more like a boundary layer in character, the temperature at the upper wall of the slot asymptotes to 0.5, consistent with (6); this equals the wall temperature in the no-flow case $\epsilon = 1$.

3.2 *The unstable temperature distribution*

When $G < 0$, $R > 0$ and so the background temperature field is destabilizing, with cold fluid overlying hot fluid. In this case, the flow tends to further distort the isotherms from the horizontal (figure 5*b*); as a result, the flow extends across the whole slot (figure 5*a*). As R increases and the lengthscale of the flow becomes smaller than the width of the slot, this flow will become unstable.

In figure 5(*c*) the temperature at each side of the slot is predicted to become infinite as $|\gamma|$ is increased just beyond 1.65. Also, in figure 5(*a*) it may be seen that as $|\gamma| = |(-R\sin^2\phi)^{\frac{1}{4}}|$ increases towards this critical value, the magnitude of the velocity diverges. However, we note that figures 5(*a*)–5(*c*) show that the velocity and temperature fields are very weak for $|\gamma| < 1.5$ (i.e. $R\sin^2\phi < 0.5$).

The one-dimensional steady solution breaks down at this critical point $\gamma \approx 1.67$ because at this point the Rayleigh number equals that of the lowest steady Rayleigh–Bénard convection mode of zero along-slot wavenumber. This follows from

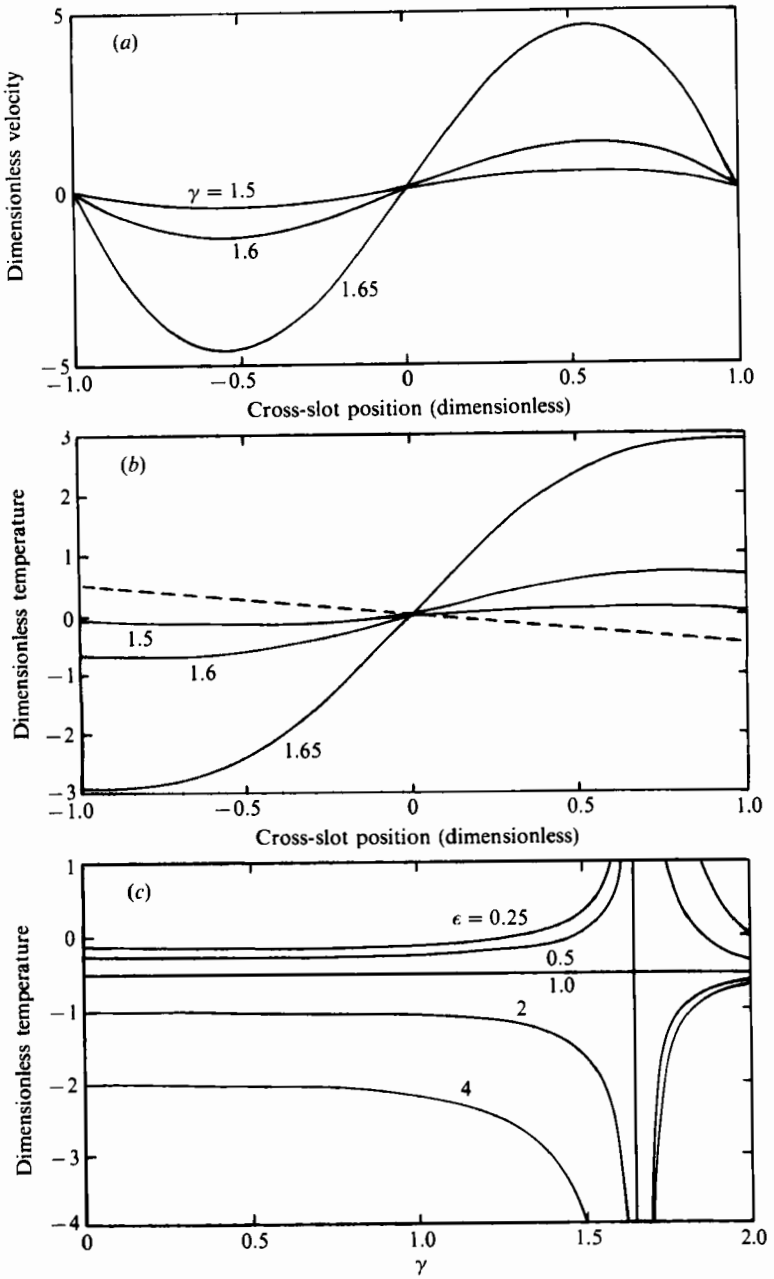

FIGURE 5. (*a*) The velocity profile when $G < 0$ with $\gamma = 1.5 \times (-1)^{\frac{1}{4}}$, $1.6 \times (-1)^{\frac{1}{4}}$ and $1.65 \times (-1)^{\frac{1}{4}}$ with $\epsilon = 0.5$. (*b*) The temperature profiles corresponding to (*a*); and (*c*) the variation of the temperature at the end of the slot, $\hat{\eta} = 1.0$, as $|\gamma|$ is increased form $\epsilon = 0.25$, 0.5, 1.0, 2.0, 4.0 with sgn $(G) < 0$.

consideration of the one-dimensional homogeneous problem described by the equations (cf. (3) and (4))

$$-\frac{\partial^2 u}{\partial t\,\partial \eta}+\nu\frac{\partial^3 u}{\partial \eta^3}=-\alpha g\frac{\partial \theta}{\partial \eta}\sin\phi, \tag{12}$$

$$\frac{\partial \theta}{\partial t}+G\sin\phi u=\kappa\frac{\partial^2 \theta}{\partial \eta^2}. \tag{13}$$

If we seek non-dimensional modes of the form

$$u(\hat{\eta})=\exp(\omega t)\,(A\sin(\lambda\hat{\eta})+B\cos(\lambda\hat{\eta})+C\cosh(\lambda\hat{\eta})+D\sinh(\lambda\hat{\eta})), \tag{14}$$

such that the velocity and heat flux vanish on either boundary ($u = u_{\hat{\eta}\hat{\eta}\hat{\eta}} = 0$), then we may add this homogeneous solution to the steady forced solution given by (5) and (6). Expression (14) satisfies these boundary conditions if $\cos(2\lambda)\cosh(2\lambda) = 1$. The lowest non-trivial eigenvalue satisfying this condition is $2\lambda \approx 4.73$. Furthermore, when $4R\sin^2\phi = \lambda^4$, there is a steady ($\omega = 0$) homogeneous solution of the form (14). The steady forced solution we have found to the original problem ((5) and (6)) coincides with this homogeneous solution whenever $\cos(2\lambda)\cosh(2\lambda) = 1$ and $4R\sin^2\phi = \lambda^4$. Therefore the steady solution first becomes singular when $R\sin^2\phi = 7.4$ (i.e. $|\gamma| = 1.67$).

The condition $R\sin^2\phi = 7.4$ (i.e. $|\gamma| = 1.67$) represents an upper bound on the stability threshold, since the flow may become unstable to two-dimensional perturbations at slightly lower Rayleigh numbers, although calculation of this stability threshold is beyond the scope of the present work.

4. Dispersion of passive tracer by the flow

Phillips (1970) calculated the convective and diffusive mass fluxes along a slot whose sidewalls are insulated. His calculation is useful, for example, in calculating the mass flux of salt along a water-filled fissure which extends from the side of a lake, in the case in which the flow along the fissure is driven by the salt gradient. However, in many situations flow may be driven by a thermal gradient, for example the geothermal gradient below the surface of the earth (Davis *et al.* 1985), yet it may be of interest to calculate the passive transport of a second component by the flow. Using the new class of thermally driven flows, which we have described in §3, we now calculate the passive transport of material along the slot. This is of interest for example in understanding how rapidly dissolved chemicals or buried (radioactive) waste products, in solution, may be dispersed along a water-saturated fracture, by the flow driven by the geothermal temperature gradient. Chemical transport is of interest when the passive chemical reacts with the rock; if the convective transport of the chemical exceeds that of molecular diffusion, then the reaction front may extend far ahead of that predicted by molecular diffusion.

As passive material of concentration $C(\eta, \xi)$ is dispersed by the flow along a narrow fracture, it may eventually reach a quasi-steady, leading-order balance between along-slope advection and cross-slope diffusion (Taylor 1953). In general, the mean concentration of passive material, $\bar{C}$, which is defined to be

$$\bar{C}=\int_{-d/2}^{d/2} C(\eta,\xi)\,\mathrm{d}\eta \tag{15}$$

is governed by the relation

$$\frac{\partial \bar{C}}{\partial t} = D\frac{\partial^2 \bar{C}}{\partial \xi^2} - \frac{\partial \overline{uC'}}{\partial \xi} \approx (D + D_T)\frac{\partial^2 \bar{C}}{\partial \xi^2} = D_{\text{eff}}\frac{\partial^2 \bar{C}}{\partial \xi^2}. \tag{16}$$

In (16), the effective diffusivity D_{eff} is the sum of the molecular diffusivity, D, and the dispersion coefficient, D_T, resulting from the shear flow, and $C = \bar{C} + C'$ where

$$C'(\eta) = \frac{1}{D}\frac{\partial C}{\partial \xi}\left[\int^{\eta}\int^{\eta'} u(\eta'')\,\mathrm{d}\eta''\,\mathrm{d}\eta' - A\eta\right]. \tag{17}$$

In (17), A is found using the condition that $\partial C/\partial \eta = 0$ at $\eta = \pm\frac{1}{2}d$, following the method of Taylor (1953). Using the flow solution (5) together with (16) and (17) one may show that

$$D_T = \frac{\kappa^2}{D}(\epsilon - 1)^2 \cot^2\phi E(\gamma), \tag{18}$$

where

$$E(\gamma) = \frac{-A(\gamma) + B(\gamma)}{16\gamma(\sin 2\gamma + \sinh 2\gamma)^2}, \tag{19}$$

with

$$A(\gamma) = 5[2\sin 2\gamma \cosh 2\gamma - 2\cos 2\gamma \sinh 2\gamma + \sinh 4\gamma - \sin 4\gamma] \tag{20}$$

and

$$B(\gamma) = 4\gamma(6\sin 2\gamma \sinh 2\gamma + \cosh 4\gamma - \cos 4\gamma). \tag{21}$$

It follows from (10*b*) that as $\phi \to 0$ or $\frac{1}{2}\pi$, for fixed Rayleigh number R, or as $\gamma \to 0$, the flow becomes very weak; hence, $D_T \to 0$ and the molecular diffusion becomes dominant. In fact, when R is small, corresponding to a weak forcing, it may be shown that (18) asymptotes to the expression

$$D_T \approx \frac{32\kappa^2(1-\epsilon)^2\gamma^8 \cot^2\phi}{2835D} = \frac{8\kappa^2(1-\epsilon)^2 R^2 \sin^2(2\phi)}{2835D}. \tag{22}$$

The dependence of the dispersion coefficient D_T upon κ^2/D may be readily understood by noting that in the present natural convective flow, given by (5), $u \sim \kappa\gamma/d$, but Taylor (1953) has shown that the shear dispersion, D_T, generally scales as d^2u^2/D. In the limit of weak forcing, $|R| \ll 1$, expression (22) suggests that the dispersion coefficient is independent of the direction of the temperature gradient, G. This is essentially because in this case the flow in the slot is linearly proportional to G (equation (5)). Also note that (22) suggests that D_T is symmetric about $\phi = \frac{1}{4}\pi$.

In figure 6(*a*) we have plotted $\cot^2\phi E(\gamma)$, where $E(\gamma)$ is given by (19), as a function of $|R|$ ($G > 0$, stable, dotted line; $G < 0$, unstable, solid line) in the case $\phi = \frac{1}{4}\pi$. This represents the dimensionless dispersion coefficient for the flow, as given by (18). From the figure, it may be seen that when there is a stable temperature gradient, if $|R| > 3$ then $E(\gamma) > 0.01$ and that $E(\gamma) \to 0.5$ as $\gamma \to \infty$. We also note that in an unstable temperature field, the dispersion coefficient is comparable to, although somewhat larger than, that for the stable flow if $|R| < 10$. This is a result of the fact that in the unstable temperature field, the flow extends right across the slot. From § 3, we expect the flow to become unstable when the Rayleigh number is of order 10. However, for larger Rayleigh numbers, when the flow does become unstable and two-dimensional, the along-slot transport will be smaller than the steady flow estimate.

For the case of a stable background temperature field, we have investigated the dependence of the dispersion coefficient upon the angle of tilt. In figure 6(*b*) we show how $\cot^2\phi E(\gamma)$ varies with slot angle for a range of magnitudes of the Rayleigh number. For each slot angle, the dimensionless dispersion coefficient asymptotes to $0.5\cot^2\phi$ as $|R| \to \infty$. Therefore, the maximum dispersion coefficient for a given

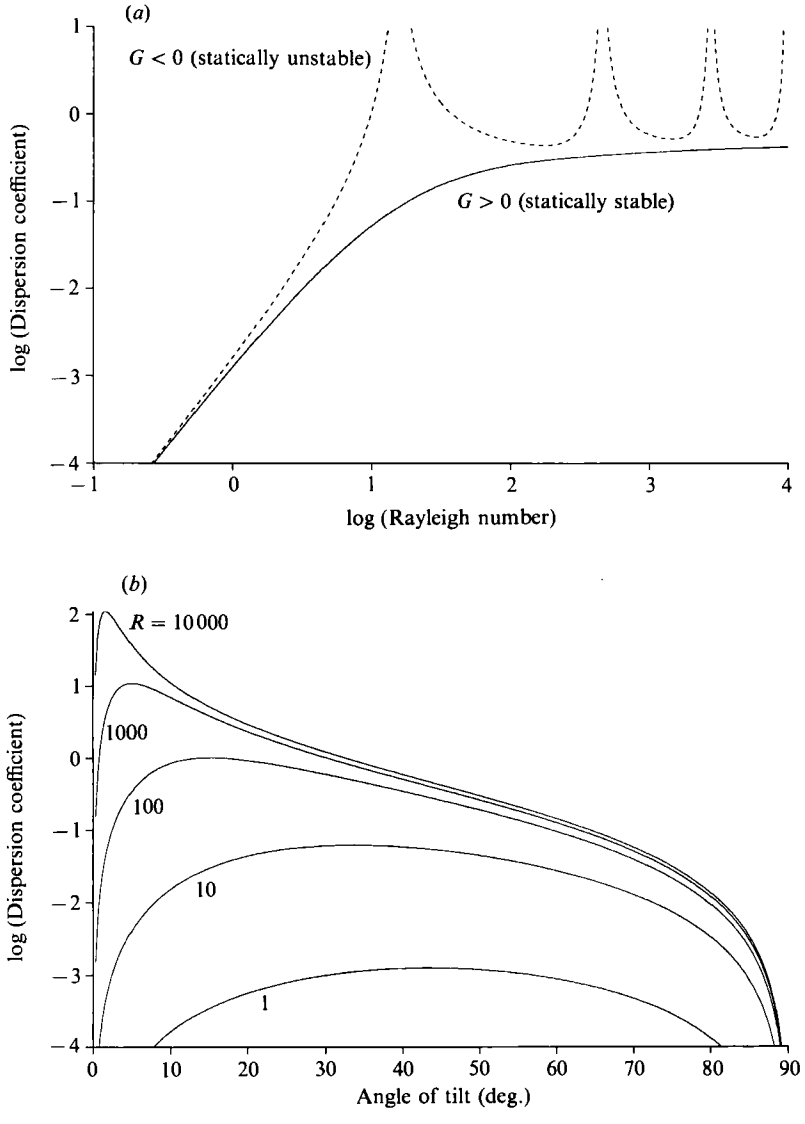

FIGURE 6. (*a*) The dependence of the dispersion coefficient, D_T, upon the magnitude of Rayleigh number $|R|$ for $G > 0$ (solid, $R < 0$) and $G < 0$ (dotted, $R > 0$) background temperature field; here the slot has angle of tilt $\frac{1}{4}\pi$. (*b*) The dependence of the dispersion coefficient upon the slot angle of tilt for $|R| = 10000, 1000, 100, 10, 1$.

Rayleigh number occurs at smaller and smaller slot angles as the magnitude of the Rayleigh number increases.

This result is particularly interesting if one considers a random network of water-filled fractures of different angles of tilt; if a passive tracer is released from a point then for weak forcing (small $|R|$), the tracer tends to travel at quite large angles to the horizontal and will be dispersed over a wide range of angles; in contrast, at much larger forcings, the tracer will tend to travel most rapidly at shallower angles to the horizontal. Therefore, with a larger thermal forcing, a tracer will tend to be dispersed through a random array of fractures over a wider horizontal area.

In figure 7, we illustrate this angular dependence of the dispersal with a plot of

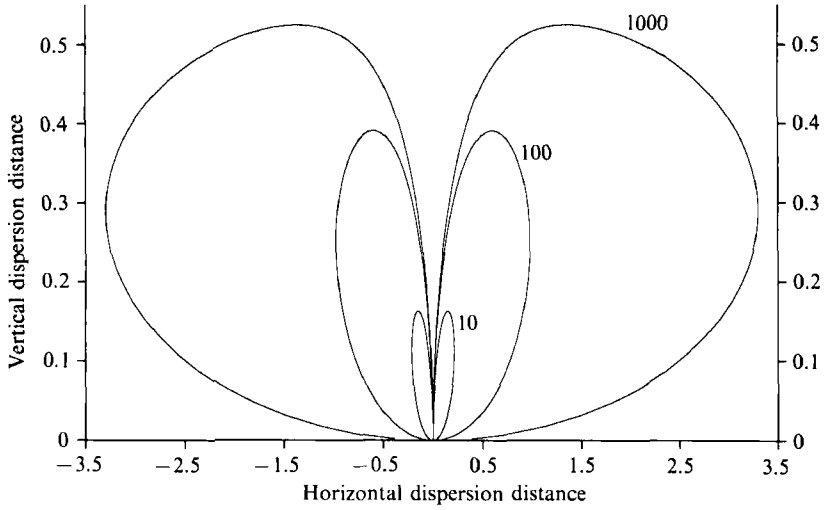

FIGURE 7. Hypothetical surfaces of a fixed concentration of contaminant at unit time after release from a point source into a medium containing an array of fractures originating at the source and orientated at different angles of inclination. Curves, $y(x)$, defined as $D^{\frac{1}{2}}(x, y) = ((D_T(\theta)\cos\theta)^{\frac{1}{2}}, (D_T(\theta)\sin\theta)^{\frac{1}{2}})$, are given for $D_T = 10D$, $100D$ and $1000D$. Note the different scales on the horizontal and vertical axes, which implies that the mean horizontal dispersal distance is very large compared to the mean vertical dispersal distance.

$((D_T\cos\theta)^{\frac{1}{2}}, (D_T\sin\theta)^{\frac{1}{2}})$. Curves are given for several values of the Rayleigh number, R, emphasizing the change in angular dependence of D_T with R. These curves represent hypothetical surfaces of fixed concentration of contaminant at unit time after release from a point source into a medium containing an array of fractures orientated at different angles. This figure identifies the strong angular dependence of the dispersion; it is remarkable that material will be dispersed most rapidly along inclined paths. As a result, material could first surface at some radial distance from the source, before it appears on the surface at points close to the source. This effect is particularly pronounced at higher Rayleigh numbers.

We now consider a specific example of dispersion along a water-filled fracture.

4.1. *Dispersion in a rock fracture*

For many passive tracers, $D/\kappa \sim 10^{-2}$; therefore, (18) and figure 6 imply that, for $\gamma \geqslant 1$, the dispersion of material along the slot far exceeds the transport by molecular diffusion. For example, in a water-filled fracture in the upper surface of the earth, $\nu \sim 0.05$ cm^2/s, $\kappa \sim 0.001$ cm^2/s, $D \sim 10^{-5}$cm^2/s, $G = -2.5\times10^{-4}$ K/cm, $\epsilon \sim 1.5$–3.0 and $\alpha \sim 0.001$. Equation (7) thus implies that $R \sim 10^{-1}d^4$ for a fracture of tilt angle ϕ. Also, in such a water-filled rock fracture, $\kappa^2(1-\epsilon)^2/D \sim 1$. Therefore, for fractures in which $d \ll 1$ cm, $\gamma \ll 1$ and the asymptotic expression (22) is valid; in this case $D_T \sim d^8 D\sin^2 2\phi \ll D$ and is therefore negligible. However, in wider fractures, in which $d > 1$ cm and $R \sim O(1)$, D_T is given by (18). From figure 6(*a*) we deduce that for $R \sim O(1)$ and $\phi \sim \frac{1}{4}\pi$, $10^{-2} \gtrsim E(\gamma) \gtrsim 10^{-3}$ and so

$$10^{-3} \leqslant D_T \leqslant 10^{-2} \tag{23}$$

which is 2–3 orders of magnitude greater than the molecular diffusion, D. Consideration of this natural convective flow is therefore crucial in determining the rate of spread of passive contaminants or tracer in wide fractures.

4.2. *Dispersion of a radioactively decaying contaminant*

We now consider how rapidly a radioactively decaying material, with radioactive concentration C per unit mass, is dispersed. In a narrow fracture the lengthscale and hence timescale of adjustment to the steady dispersive situation will be short compared to the half-life of a radioactively decaying material. Therefore, as the radioactive fluid moves along the slot, it will decay according to a conservation equation of the form

$$\frac{\partial \overline{C}}{\partial t} = -\lambda \overline{C} + (D_T + D)\frac{\partial^2 \overline{C}}{\partial \xi^2}, \tag{24}$$

where λ is the decay rate of the material. In this case, the concentration of radioactive material along the slot, in the region $\xi > 0$, originating from a decaying source of strength C_0 at $t = 0$ in the region $\xi < 0$, has the form

$$\overline{C}(\xi, t) = \overline{C}_0 \exp(-\lambda t)\operatorname{erfc}\left(\frac{\xi}{2((D_T + D)t)^{\frac{1}{2}}}\right). \tag{25}$$

Therefore if the radioactive material travels along the fracture from $\xi = 0$ to the surface at $\xi = H$, then the concentration reaching the surface at time τ will be

$$\overline{C}(H) \sim \overline{C}_0 \exp(-\lambda \tau)\operatorname{erfc}\left(\frac{H}{2((D + D_T)\tau)^{\frac{1}{2}}}\right). \tag{26}$$

We deduce that the concentration of the radioactive material at a distance H from the source will only be negligible if $H^2 > 4(D + D_T)/\lambda$. If $D_T \gg D$, then the natural dispersion transports radioactive material a factor $(D_T/D)^{\frac{1}{2}}$ further than molecular diffusion before the material has decayed radioactively.

For example, in figure 8(*a*), we show how the concentration of the material 100 m along the fracture varies with time. Each curve corresponds to a different value of D_T/D, the enhanced dispersion coefficient. We assume the material has a half-life of approximately 10^4 years ($\lambda = 10^{-11}$). It may be seen that after a few half-lives the material has decayed radioactively. For larger dispersion coefficients, the material travels further from the source before it decays and so the maximum concentration attained 100 m from the source is larger. Such a flow may therefore have an important role in pollutant transport. In figure 8(*b*), we show the concentration of tracer as a function of time at three different positions along the fracture (1, 10 and 100 m) with $D_T = 100D$. Although the decay time is independent of distance, the magnitude of the contaminant concentration and the time during which any point along the fracture is exposed to such concentrations decreases quite rapidly with distance.

From figures 8(*a*) and 8(*b*) we deduce that an increase in the dispersion coefficient can cause greater concentrations and also greater time of exposure to such concentrations at positions further from the source. In a real situation, there will be a complex network of fractures causing dispersal patterns of the form of figure 7 (assuming fracture widths are similar at all angles). As a result, radioactive contaminant may only manage to surface at points whose lateral distance from the source is of magnitude comparable to the depth of the buried contaminant; it may decay before reaching the surface if it travels along fractures with other angles of inclination.

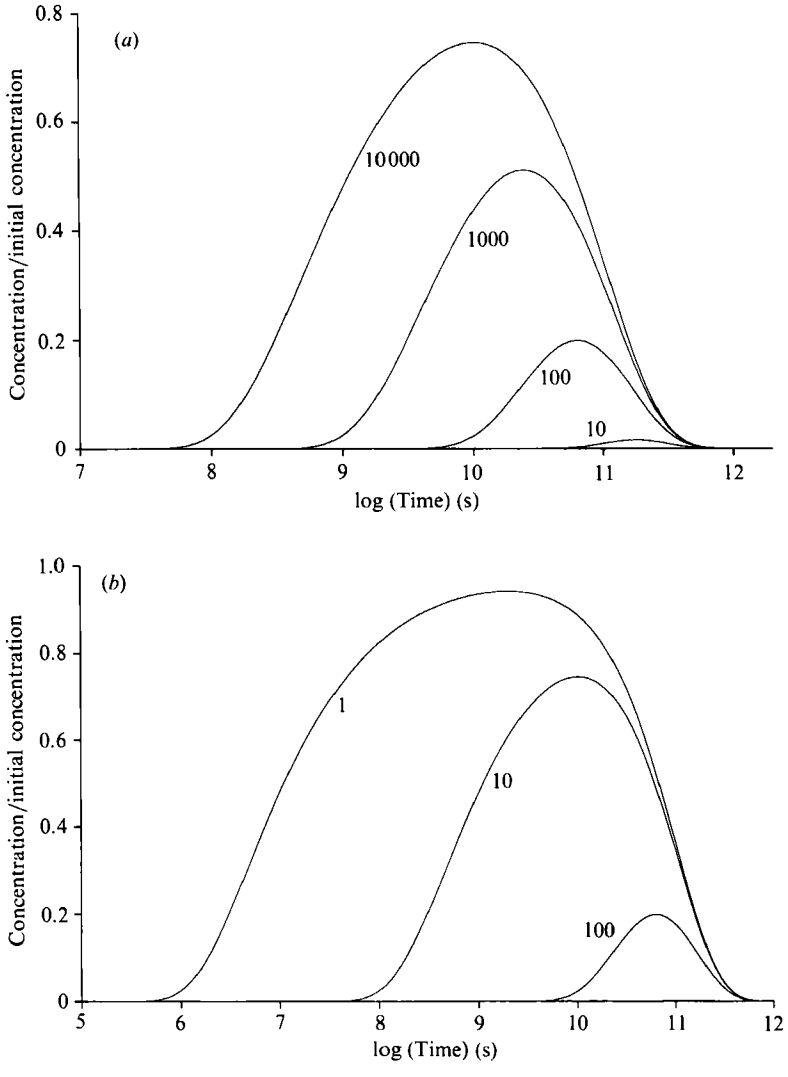

FIGURE 8. (*a*) The concentration of radioactive material as a function of time 100 m from a source. The material disperses along a fracture of inclination $\frac{1}{4}\pi$ and with dispersal coefficients $D_T/D = 10$, 100 and 1000 and 10000. (*b*) The concentration of radioactive material as a function of time 1 m, 10 m and 100 m along the fracture, of inclination $\frac{1}{4}\pi$, with $D_T/D = 100$.

5. Double-diffusive effects

Our steady-state theory may be extended to the double-diffusive situation, in which there is also a background salinity gradient along the slot, $S_{0z}\sin\phi$ (Chen 1974). However, we note cautiously that the steady solutions may now become unstable to double-diffusive instability. We include an additional equation for the conservation of salt, S, in the slot,

$$\frac{\partial S}{\partial t} + u\frac{\partial S}{\partial \zeta} = \kappa_s \frac{\partial^2 S}{\partial \eta^2}, \tag{27}$$

where κ_s is the coefficient of diffusion of salinity and S the salt concentration.

In steady state, we may combine (27) with (3) and (4), to obtain the generalized steady solution. It may be shown that the parameter γ, introduced in (10*b*), is modified to new the expression

$$\gamma_d^4 = -R\sin^2\phi(1-\kappa S_{0z}\beta/\kappa_s G\alpha), \tag{28}$$

where κ_s is the diffusivity of the salt and $\beta\rho_0 = \partial\rho/\partial S$. Furthermore, using this new scaling, γ_d, for the cross-slot variation of the forced flow solutions, it may be shown that the velocity field is of the form (5) but now with a pre-multiplying factor $[8\kappa(\epsilon-1)+\kappa_s(\beta S_{0z}/\alpha G))]/d$. The salinity satisfies an equation of the form (6), with the term proportional to $G(\epsilon-1)$ replaced by an equivalent term proportional to $-S_{0z}$. This is an extension of the work of Chen (1974), who considered the case of zero flux of both heat and salt at each bounding wall, whereas we have admitted solutions with a net heat flux at each wall. We also allow both statically stable and unstable salinity and temperature fields.

We see that the salinity can act in parallel or in opposition to the temperature field, and that the direction of flow is determined by the sign of $[\kappa(\epsilon-1)\alpha G-\kappa_s\beta S_{0z}]$. A zero-flow steady solution exists if the salinity and temperature perturbations to the density exactly balance at the boundary; however, this solution may become unstable to double-diffusive instability owing to the difference in the diffusion coefficients of salt and heat.

It readily follows from the above discussion and §4 that for a steady stable double-diffusive flow, the Taylor dispersion coefficient has value

$$D_T = \frac{32(\kappa(\epsilon-1)+\kappa_s(\beta S_{0z}/\alpha G))^2\gamma_d^8\cot^2\phi}{2835D}. \tag{29}$$

Therefore double-diffusive effects may either enhance or reduce the net dispersion of tracer.

However, we note that this double-diffusive system may be unstable. It follows from our earlier analysis that when γ_d, as defined in (28), takes the critical value ~ 1.67, the forced flow coincides with the lowest steady Rayleigh–Bénard convective mode of zero along-slot wavelength, and thus becomes singular, as in the case of one-component convection. However, the system also admits double-diffusive instabilities due to the difference in the rate of diffusion of solute and temperature. In the present problem of fixed-flux boundary conditions the full-diffusive stability analysis is non-trivial, and would form an interesting extension of the present problem. Nonetheless, our expression (29) for the dispersion of tracer represents an upper bound.

6. Conclusions

In summary, we have shown that a natural convective flow is always produced in a tilted slot when there is an imposed, vertical temperature gradient and a difference in the thermal conductivity between the fluid filled layer and the surrounding solid. The flow arises even if the density field associated with the temperature gradient is stable.

The shear dispersion associated with this flow scales as

$$D_T = 8\kappa^2\sin^2 2\phi(1-\epsilon)^2R^2/2835D, \tag{30}$$

when the slot Rayleigh number $|R| \ll 1$, but for $|R| > 1$ the dispersion coefficient may be of magnitude $D_T \sim O(\kappa^2(1-\epsilon)^2)/D$. In general this is much greater than the molecular diffusion coefficient D. For each angle of tilt, the dispersion coefficient asymptotes to a fixed value as the Rayleigh number is increased, and this value decreases with angle of tilt. As the Rayleigh number increases, the angle at which the dispersion coefficient is a maximum decreases. Thus in an array of fractures oriented at different angles, passive material will tend to be dispersed further laterally as the Rayleigh number is increased (figure 7).

We have shown that in a water-filled fracture near the surface of the earth, the dispersion coefficient, D_T, may be 2–3 orders of magnitude larger than the molecular diffusion coefficient if the rock fracture is wider than about 1 cm. We have shown that this dispersion may enable contaminants, such as buried radioactive waste, to travel one–two orders of magnitude further along the fracture before decaying radioactively. Although the real situation is more complex, in some situations, this process may reduce the surfacing time of radioactive material below its half-life.

Double-diffusive effects due to the presence of a salinity gradient along the slot modify the steady flow and can lead to an increase or decrease in the net flow and dispersion of contaminant along the slot; however, in this case double-diffusive instabilities may develop leading to a change in the flow and a reduction in the transport.

In conclusion, we mention that similar processes may also arise in water-saturated porous layers in which case the flow may be modified by slow diagenetic reactions (Davis *et al.* 1985; Phillips 1991; Linz & Woods 1992).

S. L. and A. W. W. both acknowledge support from the Summer Study Program in Geophysical Fluid Dynamics at the Woods Hole Oceanographic Institution, 1990, where this work was commenced. S. L. also acknowledges support from Deutsche Forschungsgemeinschaft. A. W. W. also acknowledges support from the Green Foundation, Scripps Institution of Oceanography where he worked on this problem as a Green Scholar. Professor S. Davis, Professor H. E. Huppert and Dr J. Lister gave some useful comments on an earlier draft.

REFERENCES

Bjorlykke, K. 1989 *Sedimentology and Petroleum Geology*. Springer.

Chen, C. F. 1974 Double-diffusive convection in an inclined slot. *J. Fluid Mech.* **72**, 721.

Davis, S. H., Rosenblat, S., Wood, J. R. & Hewitt, T. A. 1985 Convective fluid flow and diagenetic patterns in domed sheets. *Am. J. Sci.* **285**, 207.

Linz, S. J. & Woods, A. W. 1992 Natural convection, Taylor dispersion and diagenesis in a porous tilted layer. *Phys. Rev.* (submitted).

Phillips, O. M. 1970 On flows induced by diffusion in a stably stratified fluid. *Deep-Sea Res.* **17**, 435.

Phillips, O. M. 1991 *Flow and Reactions in Permeable Rocks*, pp. 1–285. Cambridge University Press

Taylor, G. I. 1953 Dispersion of soluble matter in soluble matter in solvent flowing slowly through a tube. *Proc. R. Soc. Lond.* A **219**, 186.

Woods, A. W. 1991 Boundary-driven mixing. *J. Fluid Mech.* **226**, 625.

Wunsch, C. 1970 On oceanic boundary mixing. *Deep-Sea Res.* **17**, 293.